NOTICE

CERTAIN DATA CONTAINED IN THIS DOCUMENT MAY BE DIFFICULT TO READ IN MICROFICHE PRODUCTS.

CONF-890440--1

RFP--4453

DE91 006965

SURFACE PREPARATION EFFECTS ON GTA WELD PENETRATION IN JBK-75 STAINLESS STEEL

R.D. Campbell, C.R. Heiple, P.L. Sturgill, A.M. Robertson, R. Jamsay

---

R.D. CAMPBELL, P.L. STURGILL, A.M. ROBERTSON, and R. JAMSAY are with the Joining Technology Branch and C.R. HEIPLE is with the Materials Technology Branch, EG&G Rocky Flats Plant, Golden, CO.

Paper presented at the 70th Annual AWS Meeting, held April 2-7, 1989, in Washington, D.C.

Wire Brushing of Weld Grooves Alters Surface Composition and Results in Dramatic Increases in Weld Penetration and Improved Arc Behavior

ABSTRACT

The results of a study are reported here on the effects of surface preparation on the shape of GTA welds on JBK-75, an austenitic precipitation hardenable stainless steel similar to A286. Minor changes in surface (weld groove) preparation produced substantial changes in the penetration characteristics and welding behavior of this alloy. Increased and more consistent weld penetration (higher d/w ratios) along with improved arc stability and less arc wander result from wire brushing and other abrasive surface preparations, although chemical and machining methods did not produce any improvement in penetration. Abrasive treatments roughen the surface, increase the surface area, and increase the surface oxide thickness. The increased weld d/w ratio is attributed to oxygen added to the weld pool from the surface oxide on the base metal. The added oxygen alters the surface-tension driven fluid flow pattern in the weld pool. Similar results were observed with changes in filler wire surface oxide thickness, caused by changes in wire production conditions.

Increasing the amount of wire brushing produces even deeper welds. However, a maximum in penetration is observed with further wire brushing, beyond which weld penetration decreases. The decrease in d/w ratio after extensive wire brushing is caused by weld pool slag formation produced by oxygen added to the molten pool in excess of the solubility limit. This slag changes the fluid flow and alters the arc. In this case, the benefits of wire brushing are mitigated by the presence of the slag.

INTRODUCTION

Variations in gas tungsten arc (GTA) weld shape have been traced to small differences in residual element content of the materials being welded. Heiple and Roper [1] proposed that GTA weld pool shape is determined largely by fluid flow patterns in the weld pool. The dominant force driving weld pool fluid flow, under normal GTA welding conditions, is the weld pool surface tension gradient. This surface tension gradient arises from interaction of the large temperature gradient on the weld pool surface with the surface tension temperature dependence. Surface active trace elements which segregate to the liquid metal surface lower the surface tension, thereby modifying the surface tension gradient. This in turn changes the fluid flow in the weld pool and thus the weld shape, resulting in narrower, deeper penetrating welds. This model has been described in detail elsewhere [1,2] and used to explain increased weld penetration in austenitic stainless steels when appreciable sulfur, oxygen, selenium or tellurium are present.

Oxygen is known to be surface active in iron and iron base alloys, and can increase the depth/width (d/w) ratio of GTA welds in these metals if it is not combined in stable compounds, such as aluminum oxide. The oxygen can be in the form of oxygen in the shielding gas [3,4], oxygen dissolved in the metal [2], or an oxide on the surface of the metal to be welded [2,5,6]. The amount of oxygen required under the proper conditions to produce substantial changes in GTA weld d/w ratio is very small; Heiple and Roper [2] showed a 43% increase in d/w ratio with the addition of about 15 ppm oxygen to 304L stainless steel base metal. The amount of oxygen required to produce similar increases in d/w ratio varies for different alloys.

BACKGROUND

JBK-75 is a fully austenitic, precipitation hardening stainless steel. It is a modified version of A286, the modifications being directed toward reducing the weld hot cracking tendencies of the alloy [7,8]. This material is being welded in production applications at this facility.

JBK-75, when welded using argon torch gas, is often difficult to penetrate and is not sensitive to weld parameter variations from a penetration standpoint. This poor welding behavior is compounded by the use of a deep, narrow, and asymmetrical U-groove weld joint. Welds made using this configuration resulted in marginal and inconsistent penetration. As a result, the torch gas was changed to 25% argon - 75% helium. These welds had more penetration but were accompanied by arc instability. This instability is defined as multiple stable arc lengths for a given voltage. Since these welds were controlled by automatic voltage control (AVC), the result was that the torch periodically moved up and out of this narrow weld groove, resulting in lack of penetration. Although part of this instability problem is a characteristic of helium torch gas [9,10], the use of the narrow groove caused the AVC to sense the sidewalls of the groove, which aggravated the problem. Unfortunately, the weld joint could not be modified, the Ar-He torch gas was necessary to obtain adequate penetration, and changing the alloy composition was not an option. In the course of weld development, improved penetration and arc stability were noted on wire brushed samples. This study was undertaken to verify the effect of wire brushing, to understand the origin of the increased penetration produced by wire brushing, and to see if other surface treatments would either be more effective or simpler. A variety of chemical, abrasive, and machining techniques were evaluated. Their effects on surface chemistry, penetration, and voltage-arc length relationships are discussed herein.

EXPERIMENTAL PROCEDURES

Materials

Three heats of JBK-75 bar stock were utilized in this study, the compositions of which are presented in Table 1. The materials were all produced by the vacuum induction melt/vacuum arc remelt (VIM/VAR) procedure.

Surface Preparation Methods

Numerous surface preparations were evaluated, including chemical and abrasive surface preparations, various machining methods and finishes, and various degrees of wire brushing.

Chemical and Abrasive Surface Preparation Experiments

In the initial experiments, 2-inch diameter, 1-inch thick samples of Heat

A were prepared by twelve different chemical or abrasive surface treatments to determine which, if any, affected weld shape. The various treatments are detailed in Table 2. Three general types of chemical cleaning were attempted on the steel prior to welding: acid cleaning, acid cleaning followed by solvent cleaning, and solvent cleaning. The two abrasive conditions involved wire brushing in air and grit blasting using 180 grit silica particles transported in air. The abrasive treatments were applied after acid cleaning (i.e. Condition 1A in Table 2) and were followed by a wipe with isopropyl alcohol.

Machining Experiments

The second set of experiments involved a variety of mechanical surface preparations on 6-inch diameter, 1 inch thick samples of Heat B to determine if weld penetration could be improved by surface roughening caused by different machining schedules. Surface roughness was varied by machining the surface via lathe turning, travelling wire electrical discharge (EDM), and different milling schedules. The five surface finishes achieved are listed in Table 3.

For each of the five surface finish conditions, three different treatments were evaluated: (1) the machined samples were acid cleaned (using procedure 1A in Table 2), (2) the machined samples were wire brushed, then acid cleaned, and, (3) the machined samples were acid cleaned, then wire brushed (followed by wiping with isopropyl alcohol to remove any residue from the wire brushing). These treatments are identified as Conditions A, B, and C, respectively, in Table 3. Thus, fifteen different conditions were tested.

Wire Brushing Experiments

The final set of experiments involved varying the amount of wire brushing on the flat surfaces of 2-inch diameter, 1 inch thick samples of Heat C. These experiments were performed to determine the relationship between the amount of wire brushing, oxide thickness, and weld penetration. Samples were first acid cleaned using procedure 1A (Table 2). Wire brushing was accomplished by holding the sample in a Hardinge head fixture which rotated the part under the wire brush at a constant speed (5.35 in/min - 2.3 mm/sec). The wire brush also turned at a constant speed. As the brush was lowered, it applied a constant force to the rotating sample. The amount of wire brushing is expressed as the number of times (passes) the sample was rotated under the wire brush.

The wire brushes were made of AISI 302 stainless steel, with a maximum sulfur content of 0.03% (300 ppm). All brushes were vapor degreased using procedure 3A in Table 2. Electron microscopy of the wire brushed surfaces indicated that no wire residue was embedded nor trace elements picked up from the brush.

Welding and Metallography

To properly evaluate weld pool fluid flow characteristics and subsequent weld bead geometry, partial-penetration, autogenous (no filler wire) welds were produced utilizing the GTA process.

Chemical and Abrasive Experiments

For the chemical and abrasive experiments, bead-on-plate welds were produced on both the circumference and flat surfaces of samples of Heat A using welding procedures 1 through 3 listed in Table 4. Automatic voltage control (AVC) was used on some welds (procedures 1 and 3) to maintain a constant arc voltage by adjusting torch height (position) during welding. Torch motion was recorded with a data acquisition system accurate to 0.001 in. (0.03 mm). Welds were also produced utilizing a fixed arc length of 0.066 in. (1.7 mm) between the tip of the electrode and the top of the sample (procedure 2). Arc voltages, accurate to 0.01 volt, were recorded with the data acquisition system.

Procedures 1 through 3 were used to produce one or two welds on each of the twelve surface conditions. Procedures 1 and 2, substituting 100% argon for the argon-helium shielding gas, were also utilized on several of the acid cleaned and on the wire brushed samples. Four to eight transverse cross sections were taken from each weld and depth-to-width (d/w) ratios were obtained from these sections.

Machining Experiments

For the machining experiments, both spot-on-plate and bead-on-plate welds were produced on the machined faces of samples of Heat B utilizing procedures 4 and 5 listed in Table 4. These welds were made with automatic voltage control and Ar-He shielding gas.

One spot weld was made on each of the fifteen surface treatments identified in Table 3. Spot weld diameters (widths) were measured prior to metallographic sectioning through each weld centerline, from which the maximum depths of penetration were obtained. The bead-on-plate welds were produced by making continuous (circular) welds across several surface treatments, which allowed evaluation of changes in weld shape with surface condition. Two cross sections were taken in each of the fifteen surface treatment regions to obtain weld profiles.

Wire Brushing Experiments

Bead-on-plate welds were produced with argon-helium gas on the samples for the wire brushing experiments using procedure 6 listed in Table 4. One weld was made on each flat surface of samples of Heat C, each sample having been prepared with a different amount of wire brushing. At least eight transverse cross sections were taken from each weld, and reported d/w ratios reflect the nominal values of the individual measurements.

Surface Analysis

The thickness of the oxide layers produced by various surface treatments was measured with a Surface Science Laboratory SSX-100 ESCA spectrometer. Oxide thickness was measured by depth profiling the surface, and defining the oxide thickness as the ion etching time at which the oxygen photoelectron peak area dropped to one half the maximum value. In order to convert the ion etching time to thickness, the etching rate was taken to be the same as that for SiO_2 on Si. The actual etching rate is likely to be somewhat different, but use of the SiO_2 rate provides a reasonable estimate and, in any event, relative values for the different surface treatments will be correct. It is recognized that oxide thickness measured in this way becomes less reliable as surface roughness increases. The measured oxide thickness on roughened surfaces should be taken as an indication only. Oxide thickness on certain samples was also measured by depth profiling in a PHI 590 Auger spectrometer. The results of these measurements were in agreement with the ESCA results and are included with them.

RESULTS AND DISCUSSION

Chemical and Abrasive Experiments

Weld Penetration

Abrasive surface preparations resulted in significantly deeper weld penetration than chemical surface preparations, as illustrated by the weld cross sections in Figure 1 (produced from procedure 1 with constant voltage and Ar-He shielding gas). The mean, maximum, and minimum weld d/w ratios for the twelve chemically and abrasively prepared samples produced with welding procedure 1 are plotted in Figure 2a. All ten chemical cleaning methods (shown in the same order as listed in Table 2) produced similar weld profiles, with a mean depth-to-width ratio of 0.391. In contrast, the abrasively prepared samples had significantly greater d/w ratios. The wire brushed samples produced a depth-to-width ratio of 0.660, and the grit blasted samples had an average d/w ratio of 0.848, more than twice that of the chemically cleaned samples.

Similar weld profiles were produced when a fixed arc length was maintained. Comparison of Figures 2a and 2b illustrates that the d/w ratios for the chemically prepared samples were essentially constant regardless of whether a constant voltage (Figure 2a) or a fixed arc length (Figure 2b) was maintained. The abrasively prepared samples also had the same weld profiles with either constant voltage or fixed arc length. The difference in weld profile between chemically and abrasively prepared samples was unchanged when Ar-He shielding gas was replaced with 100% argon.

Welds produced on the circumferences using constant voltage and pure argon also produced similar weld profiles (compare Figure 2c with Figures 2a and 2b). These figures illustrate that the increased weld penetration on the abrasively-prepared samples occurs regardless of voltage/arc-length control techniques or shielding gas composition.

Surface Aralysis

The increase in weld penetration was related to surface oxide thickness. As illustrated in Figure 2d, the measured surface oxide thickness was essentially the same following the various cleaning treatments. However, the oxide thickness was increased substantially by wire brushing, from 14-25 Angstroms for chemically-prepared surfaces to 40 Angstroms for the wire brushed sample. Wire brushing, in addition, increases the surface area by increasing the surface roughness, and oxide is also folded mechanically into the surface. It is postulated that when a weld is produced on the wire brushed (or grit blasted) surface, more oxygen enters the weld pool. Surface tension gradients are altered, and the fluid flow pattern changes to produce a deeper, narrower weld bead

Arc Voltage-Arc Length Relationships

Measurements of arc lengths and arc voltages (made during welding with procedures 1 and 2 using both gases) resulted in the average values illustrated in Figure 3. For the welds made with Ar-He using constant voltage, there was only a slight decrease in nominal arc length (0.003 in.) for the abrasively treated samples compared with the chemically treated samples (compare Point B to Point A in Figure 3). Likewise, when a fixed arc length was utilized, the average arc voltage increased only slightly (0.03 volts) with the abrasive treatment (compare Point D to Point C in Figure 3).

As illustrated in Figure 3, the weld d/w ratios for these same samples increased by nearly 100%. For the welds in which the arc length decreased by 0.003 in., the d/w ratio increased from 0.391 to 0.754 (Cross sections A and B). For the welds in which the voltage increased by 0.03 V, the d/w ratio increased from 0.390 to 0.745 (Cross sections C and D). The shifts in arc voltage and arc length are minor and are well within the calibration limits of the equipment. Neither the decrease in arc length nor the increase in arc voltage could possibly account for the observed, dramatic increase in penetration. Thus, the increase in penetration is not caused simply by a change in arc characteristics.

The abrasive treatment produced a shift of the voltage-arc length curve upward and to the left when 100% argon shielding gas was used (Figure 3). This shift consisted of a decrease of 0.011 in. in arc length (compare Points F and E) and an increase of 0.72 volts (compare Points H and G). The d/w ratios for the abrasively-prepared samples were greater than for the chemically-prepared samples (compare cross sections F to E and H to G), but the increase was not as large as with the Ar-He gas.

With 75% helium, arc characteristics are dominated by the higher thermal conductivity and higher ionization potential of the helium gas and there is less effect of the abrasive treatment (i.e. oxygen content) on the arc voltage or arc length. However, in argon, abrasive treatment changes the arc length - arc voltage relationship significantly, as evidenced by a shift of 0.72 volts.

Torch Motion/Voltage Variation

Overall torch motion during welding on the solvent cleaned only and abrasively prepared samples (with constant voltage and Ar-He gas) was approximately 54% less than on the acid cleaned samples. Variations in arc voltage during welds with fixed arc length were also significantly lower for the solvent cleaned only and abrasively treated samples, by approximately 0.3 volt for the Ar-He gas and 0.1 volt for the argon gas. These reduced variations in both arc voltage and torch motion during welding on the solvent cleaned only and abrasively treated samples are important, especially considering the deep, narrow U-groove used in production. The wire brushed, grit blasted, or solvent cleaned surfaces produce a more stable welding arc (i.e. less arc wander); thus, the AVC does not sense off the sidewalls. During production welding this allows the torch to remain in the groove without climbing up and out. The result is a deeper and more consistent full-penetration weld.

The composition of the surface oxide after acid cleaning differed from that following abrasive treatment or solvent cleaning. Acid cleaning produces a passivated surface enriched in chromium and titanium compared to surfaces oxidized in air. Abrasive treatment following acid cleaning removes the thin passive oxide and leaves a typical air-oxidized surface. The difference in oxide composition appears responsible for observed changes in arc stability.

Summary: Chemical and Abrasive Experiments

The chemical and abrasive preparation experiments thus showed that abrading the surface dramatically increases weld penetration compared with the ten chemical treatments. This apparently was caused by a thicker oxide combined with increased surface area, which allows more oxygen to enter the weld puddle and alter fluid flow characteristics. The increase in penetration was not caused by an increase in heat input from a higher arc voltage or a shorter arc length. Decreased arc stability on acid cleaned surfaces is apparently caused by the passive oxide formed by this treatment.

Machining Experiments

Measurements of the maximum spot weld penetrations and spot weld diameters resulted in the depth-to-width ratio curves illustrated in Figure 4. Spot welds on all machined-plus-acid cleaned samples (Conditions A) produced d/w ratios ranging from 0.400 to 0.435. On the machined, wire brushed and acid cleaned samples (Conditions B) the welds had similar profiles, with d/w ratios ranging from 0.390 to 0.417. However, all welds made on the regions which were machined, acid cleaned, then wire brushed (Conditions C) had significantly (19.2%) greater d/w ratios (0.475 to 0.494) than welds made on either of the other two conditions, regardless of machined surface roughness. This was a result both of an average increase in penetration of 8.8% and also an average decrease in weld bead diameter (width) of 8.4%.

Differences in penetration behavior with surface roughness are minor in comparison to the differences observed when the surface was wire brushed as the final operation prior to welding (Figure 4). Surface roughness measurements of the wire brushed samples were similar regardless of whether they were brushed before or after acid cleaning (wire brushed surfaces were rougher than as-machined surfaces). Therefore, the increase in depth-to-width ratio was caused by the microscopic abrasion produced by wire brushing rather than by macroscopic roughening produced by machining.

Bead-on-plate welds showed similar welding responses. Weld cross sections from bead-on-plate welds on the surface with a 125 microinch finish are shown in Figure 5. The weld profile for the sample which was machined, acid cleaned, and wire brushed (Figure 5c) is deeper and narrower than for the other two conditions with the same surface finish (Figures 5a and b).

Depth-to-width ratios increased dramatically from 0.392-0.395 for the samples which were acid cleaned after machining (and wire brushing) to 0.626 for the sample which was wire brushed after the cleaning operation.

Depth-to-width ratios on spot welds and bead-on-plate welds were similar for Conditions A and B. However, the d/w ratio for Condition C (i.e. wire brushed as the final operation before welding) was significantly greater for the bead-on-plate weld (0.626) compared with the spot weld (0.490). This difference is most likely a result of differences between stationary and travelling welds.

One important difference between stationary and traveling welds is that the weld pool surface temperature reached in stationary welds exceeds that in traveling welds [11]. Trace element effects should therefore be less pronounced in stationary welds because a larger portion of the pool surface is above the temperature range where a positive surface tension temperature coefficient exists [12]. In addition, for a spot weld on a material where the surface active elements are present largely on the surface of the base metal, the weld pool consumes a continuously decreasing ratio of surface active element to volume as the weld pool grows.

Although there is some variation in penetration with machined surface finish, in all cases the samples which had been wire brushed as the final operation prior to welding produced the highest depth-to-width ratios. Wire brushing substantially increases the amount of oxygen on the surface because of increased oxide thickness, increased surface area (from micro-roughness), and mechanical folding of oxide into the surface. This combined increase is much larger than from differences in machined surface finish.

Wire Brushing Experiments

Weld Penetration/Arc Behavior

Weld d/w ratio was a strong function of the amount of wire brushing. A plot of weld d/w ratio versus amount of wire brushing is shown in Figure 6 for welds produced in Ar-He. Similar profiles were produced when welded with 100% argon, only with lower d/w ratios.

Figure 6 also shows that wire brushing only changes weld shape when the wire brushing is performed in air (or, presumably, in some other oxygen-containing atmosphere). Wire brushing in argon had no effect on subsequent weld shape and welds on all samples wire brushed in argon behaved similarly to those on unbrushed surfaces.

The change in weld shape for wire brushed samples (in air) compared to unbrushed (acid cleaned) samples is quite dramatic. Weld cross-sections from four conditions are shown in Figure 7. The increase in d/w ratio is approximately 50% as a result of the optimum brushing condition. The maximum in weld d/w ratio at 6-9 wire brushing passes results from both a narrowing and deepening of the weld pool, as illustrated in Figures 7 and 8. Beyond approximately 12 wire brushing passes, weld profiles are constant.

Figure 9, which illustrates the top surfaces of the same four welds shown in Figure 7, reveals several features. Weld beads become narrower and the shape of the weld bead becomes more uniform, with parallel edges, as the amount of wire brushing is increased. However, slag forms along the edges of the weld with 8 or more wire brushing passes, and the amount of slag increases with increasing wire brushing. With 50 wire brushing passes, the slag is continuous along both edges of the weld, as illustrated in Figure 9d and by the uneven top surface in Figure 7d.

It should be noted that a portion of the increase in weld d/w ratio with modest amounts of wire brushing results from a change in arc-weld pool behavior. Photographs of welds are shown in Figure 10 for unbrushed and 2 times wire brushed samples. These still photographs were taken from a videotape made during welding, utilizing a laser-enhanced vision system. A video camera senses the image of the weld puddle, and by appropriate shuttering and synchronization of an ultraviolet laser and camera, the arc light is filtered out so that only the electrode tip and weld pool are seen (a reflection of the electrode tip appears in the center of the weld pool). The photographs in Figure 10 reveal instantaneous weld pool dimensions, weld pool wander, and overall weld bead width.

The weld pool on the unbrushed sample (Figure 10a) is wide and wanders in a side-to-side and front-to-back motion. This wander is caused by the arc-weld pool interactions with the base metal surface. The weld pool sweeps out a width approximately 120% of the instantaneous pool width and the resultant weld bead, as measured by transverse cross sections, is thus wider than the actual pool. The wander produced the irregular weld bead shape illustrated in Figures 9a and 10a for the unbrushed sample.

On the sample that was brushed two times (Figure 10b), the pool became narrower - approximately 70% as wide as the unbrushed weld. The weld bead in this case is the same width as the stantaneous pool width. Weld pool wander also ceased, producing a more desirable welding performance and a uniform weld bead with parallel edges, as evidenced by the top bead appearance in Figure 9b for a sample brushed 4 times. Overall vertical torch motion decreased significantly with wire brushing, from 0.017 in. for the unbrushed samples to 0.001-0.002 in. for samples wire brushed five or more passes. The frequency of torch motion was also reduced by 50% on the wire brushed samples. On heavily brushed surfaces, particles were observed moving along the top surface of the weld pool inward toward the center, as expected from the fluid flow pattern responsible for deep penetration.

Photographs from the videotape reveal that the wire brushed surface produces two different qualitative effects. One is to reduce the width (while increasing the depth) of the weld by surface-tension driven fluid flow. The other is to increase arc stability and decrease pool wander. The increase in weld bead depth-to-width ratio is a result of both of these. The latter effect has the most significance in terms of improving welds made in grooved joints.

Arc Length

Measurements of electrode-to-work distances revealed a change in arc gap with wire brushing n air. Arc length increased slightly from 0.083 in. on the unbrushed sample to 0.096 in. on the sample brushed 3 times, then continuously decreased with further wire brushing until an arc length of 0.047 in. was achieved for the sample wire brushed 350 times (using AVC and Ar-He gas). The decrease was not correlated with slag formation.

For samples wire brushed in argon, the arc length increased slightly from 0.083 in for the unbrushed sample to 0.109 in. for the sample brushed 200 times (also using AVC and Ar-He gas). These results show that the arc length decrease was associated with increased wire brushing, but only when the brushing was performed in air. A slight decrease in arc gap was noted previously for wire brushed samples compared with chemically prepared samples (Figure 3). Decreased arc length does not cause the improved penetration observed with wore brushing, but rather may be a result of the altered fluid flow.

Surface Analysis

Wire brushing results in an increase in surface oxide thickness, as measured by ESCA and Auger depth profiling (Figure 11). The increased oxide thickness is expected from local heating under the wire brush. These results are consistent with the results from the Chemical and Abrasive Experiments.

Wire brushing produces a dull, matte finish compared with the bright, shiny surface appearance obtained by acid cleaning. There is also a substantial increase in surface roughness, as illustrated in Figure 11 and the scanning electron micrographs in Figure 12. The unbrushed surface reveals the lathe-turned finish while heavy brushing produces extensive surface lapping. Oxidized surfaces have been mechanically folded over themselves, thereby increasing the surface area. Further brushing causes more and more surface to become exposed and folded. Wire brushing in argon produced similar surface roughnesses but caused no change in surface oxide thickness from the unbrushed surface, and resulted in no change in weld penetration (see Figure 6).

The combination of increased oxide thickness, increased surface area, and oxide trapped in surface laps with more wire brushing adds oxygen to the weld pool during welding. This additional oxygen produces inward surface tension driven fluid flow, resulting in increased weld d/w ratios.

Slag Formation

For heavily brushed surfaces (greater than approximately 12 wire brushing passes), the level of oxygen apparently exceeds the solubility limit in the liquid and results in formation of weld slag on the top surface of the weld pool (see Figures 9c and d). ESCA profiling of surface slag revealed it to be nearly all titanium oxide, with minor amounts of chromium, nickel, aluminum, and nitrogen. Apparently the presence of extensive slag on the weld pool surface interferes with the arc as well as the fluid flow patterns necessary for deep penetration weld pools. This slag may impede fluid flow as well as insulate the liquid, resulting in the decreased d/w ratios for greater than approximately 12 wire brushing passes, as illustrated in Figure 8.

The behavior of weld d/w ratio with increasing wire brushing is consistent with previous measurements of the effect of torch (shielding) gas oxygen content on weld d/w ratio (Figure 13) [3]. Weld d/w ratio passes through a maximum with increasing torch gas oxygen content, and then declines.

Weld Filler Wire

Similar weld variability has been observed with differences in JBK-75 weld filler wire surface oxide. Figure 14 reveals the differences in full penetration weld profiles produced by two spools of wire made from the same heat and lot of material. Each spool of wire was cold-rolled and abrasively cleaned separately, resulting in somewhat different surface oxide thicknesses. The wire with the thicker oxide layer (133 Å) produced deeper, narrower weld puddles, which remained down in the groove and resulted in adequate underbead dropthrough. Wire lightly oxidized by heating in an air furnace also produced improved penetration.

Amount of Oxygen Added

The correlation between increasing oxide thickness and weld shape is good, but the question naturally arises as to whether there is enough oxygen in these thin oxides (particularly on weld filler wire) to conceivably alter weld pool behavior. For the 0.045 inch diameter weld wire, a simple calculation demonstrates that a 70 Å thick Cr_2O_3 layer on a perfectly smooth cylindrical surface would add about 5 ppm oxygen to the average oxygen content of the wire. However, the actual wire surface is not at all smooth, so that the real surface area is considerably larger than the geometric area calculated assuming a smooth surface. The ratio of the actual surface area to the geometric area is known as the surface roughness factor. The surface roughness factor has been measured by Maeda et al. [13] for 304 stainless steel polished to a mirror-like surface with 0.3 μm alumina. They obtained a surface roughness factor of 2.7. Prazak and Eremias [14] found a factor of 8.9 for steel, grit blasted with 0.3 mm grit. The roughness of the cold-rolled weld wire is probably similar to the grit blasted steel, so the actual oxygen contribution from a 70 Å thick oxide layer is likely to be about 45 ppm. Thus, the magnitude of the oxygen addition from the weld wire is comparable to that known [2] to cause substantial changes in weld pool shape.

The contribution of oxygen from wire-brushed surfaces, particularly in a weld groove, is even larger. Bulk chemical analysis for oxygen was performed on two samples of weld metal from each of several welds with different surface preparation. One sample included the weld bead top surface and any slag present, while the other sample did not include the surface. The samples which included the weld bead surface were 0.050 in. (1.3 mm) thick, and all samples contained only weld metal.

For samples wire brushed in air, the oxygen content of the bulk weld metal increased only slightly with increasing amounts of wire brushing (up to only 50 ppm compared with the 44 ppm oxygen base metal composition). However, samples including the weld bead surface showed substantially higher oxygen content with wire brushing, up to 180 ppm oxygen for the sample wire brushed 35 times. Thus, while some oxygen entered the bulk weld metal, most of the additional oxygen added to the weld pool as a result of wire brushing in air remained on the pool surface.

For samples wire brushed in an argon atmosphere, chemical analysis showed essentially no difference in oxygen content between the bulk weld metal and the samples including the weld bead surface. There was no increase in oxygen with increasing amounts of wire brushing. Thus, brushing in argon does not introduce appreciable oxygen into the surface.

Summary

All the observations are consistent with the addition of oxygen to the weld pool from the weld wire or base metal surface as the cause for changes in weld pool shape. Wire brushing in air increases the oxygen content of the surface and changes weld shape; wire brushing in argon does not change the surface oxygen content appreciably and does not alter weld shape. The dependence of weld d/w ratio on the amount of wire brushing is similar in form to the dependence of weld d/w ratio on oxygen additions to the torch gas. Various chemical surface cleaning treatments did not change surface oxide thickness significantly and had little effect on weld shape. A simple calculation indicates that enough oxygen is available in the surface oxides to affect weld pool shape. Slag formation on welds over heavily wire brushed surfaces demonstrates that oxygen is being added to the weld pool. A portion of the improvement in weld shape from wire brushing arises from increased arc stability and reduced pool wander. The lower arc stability on acid cleaned surfaces is apparently caused by the surface oxide enriched in chromium and titanium formed by this treatment.

Finally, it should be noted that GTA weld pool shape in JBK-75 stainless steel appears to be particularly sensitive to oxygen additions. Similar results were obtained on all three heats of JBK-75 in spite of small variations in sulfur, oxygen, aluminum, and silicon contents. Limited tests similar to those reported here have been performed on 304L, 316L, and 21-6-9 stainless steels. The results were similar to those with JBK-75, but the effects appear to be smaller and more brushing is required to produce any change.

The origin of the high sensitivity of JBK-75 stainless steel weld shape to oxygen is not known. JBK-75 is the only alloy studied which contains Ti and Al above trace levels, which might be responsible for the alloy's high sensitivity to oxygen. Another possibility is indicated by surface tension measurements on iron-silicon alloys in contact with carbon dioxide [15]. The effect of CO_2 on the surface tension was a strong function of silicon content. For low silicon alloys, the surface tension dropped sharply when contacted with CO_2. For alloys with more than 1.2% Si, the surface tension increased when contacted with CO_2. The different behavior was attributed to differences in slag formation on the liquid metal surface. Thus silicon appears to interfere with oxygen producing a positive surface tension temperature coefficient on liquid iron. The JBK-75 stainless steel used in the experiments reported here contained only about 0.06% Si, and the 21-6-9 used for the torch gas experiment (Figure 13) contained only 0.16% Si. Type 304 stainless steel typically contains more than 0.5% Si. Thus the high sensitivity of JBK-75 to oxygen additions may be related to its unusually low silicon content.

CONCLUSIONS

Small changes in the concentration of surface active trace elements in weld pools can have a substantial effect on GTA weld pool shape in high purity steels. Because the quantity of surface active material required to affect weld pool shape can be so small, it can arise from unexpected sources. Wire brushing, or other abrasive surface treatments (in air), are effective means of increasing GTAW penetration and improving arc stability, at least in JBK-75 stainless steel. Wire brushing alters the surface of JBK-75 by producing a thicker oxide layer than produced by chemical cleaning methods. Wire brushing also roughens the surface, and folds laps of oxide into the surface, thereby increasing the amount of oxide. The oxygen added to the weld pool alters fluid flow and improves penetration (d/w ratio) in accord with the surface tension driven fluid flow model proposed by Heiple and Roper. Acid cleaning JBK-75 produces an oxide layer enriched in chromium and titanium, which apparently causes significant arc instability and weld pool wander for reasons not at present understood. This thin layer is removed by wire brushing, thereby producing a more stable weld.

Increasing the amount of brushing increases the surface roughness and the oxide thickness. This causes weld penetration to increase, until the oxygen solubility limit is reached, at which time a slag forms on the surface of the weld pool. This slag affects the fluid flow and reduces weld penetration. The optimum level of wire brushing on flat surfaces occurs between 6 and 9 wire brushing passes. The optimum level will be different in a groove.

Other methods of introducing oxygen into the surface should show similar responses. Although silica grit blasting produced increased weld penetration, welding behavior was undesirable because of arc instability and excessive pool slag. These problems may be correctable with less severe grit blasting. Possible entrapment of silica in the surface was also a concern. Qualitatively similar results were obtained when oxygen was ion implanted on JBK-75. Heat treatment to grow an oxide, or any other method to introduce oxygen to the surface should also work. Surface alteration may be an acceptable method to increase, or at least control, weld penetration.

ACKNOWLEDGMENTS

The authors wish to acknowledge the contributions of V.J. Lusero, R.L. Page, R.W. Sakaguchi, D.K. Thistlewood, and D.R. Watson of the EG&G Rocky Flats Plant, who performed some of the wire brushing and welding experiments detailed in this study. B.J. Smith, D.T. Larson, C.A. Perkins, and J.C. Petersell provided support in the chemical cleaning experiments and Auger electron microscopic analysis areas. This work was supported by the United States Department of Energy, Albuquerque Operations Office. Their support is gratefully acknowledged.

REFERENCES

1. Heiple, C.R. and Roper, J.R. 1982. Mechanism for minor element effect of GTA fusion zone geometry. *Welding Journal* 61(4): 97-s to 102-s.

2. Heiple, C.R. and Roper, J.R. 1982. Effects of minor elements on GTAW fusion zone shape. *Trends in Welding Research in the United States*, S.A. David, ed., pp. 489-520, American Society for Metals, Metals Park, Ohio.

3. Heiple, C.R., Burgardt, P., and Roper, J.R. 1984. The effect of trace elements on GTA weld penetration. *Modeling of Casting and Welding Processes II*, J.A. Dantzig and J.T. Berry, eds., pp. 193-205, TMS-AIME, Warrendale, PA.

4. Starr, J.W., Campbell, R.D., and Henningsen, J.L. 1990. Unpublished research, EG&G Rocky Flats, Golden CO.

5. Majetic, J.C. and Yeo, R.B.G. 1971. Method of welding stainless steel. U.S. Patent 3,584,187.

6. Campbell, R.D. 1987. *An investigation into the physical metallurgy, welding metallurgy, hot-cracking and weld pool shape of ferritic stainless steels.* PhD Thesis, Rensselaer Polytechnic Institute, Troy, NY.

7. Brooks, J.A. and Krenzer, R.W. 1974. Progress toward a more weldable A-286. *Welding Journal* 53(6): 242-s to 245-s.

8. Brooks, J.A. 1974. Effect of alloy modifications on HAZ cracking of A-286 stainless steel. *Welding Journal* 53(11): 517-s to 523-s.

9. Morton, H.S. and Gage, R.M. 1956. Arc properties in the five rare gases. *Arcs in Inert Atmospheres and Vacuum*, W.E. Kuhn, ed., pp. 8-18, The Electrochemical Society, New York, NY.

10 Lancaster, J.F. 1986. The electric arc in welding. *The Physics of Welding*, Second Edition, J.F. Lancaster, ed., pp. 146-227, International Institute of Welding, Oxford, U.K.

11. Zacharia, T., David, S.A., Vitek, J.M., and Debroy, T. 1989. Weld pool development during GTA and laser beam welding of type 304 stainless steel, Part I - Theoretical analysis. *Welding Journal* 68(12): 499-s to 509-s.

12. Heiple, C.R. and Burgardt, P. 1990. Penetration in GTA welding. *Weldability of Materials*, eds. R.A. Patterson and K.W. Mahin, pp. 73-80, ASM International, Materials Park, OH.

13. Maeda, S., Mohri, M., Hashiba, M., Yamashina, T., and Kaminsky, M. 1981. Surface roughness factor measurements of 304 and 316 stainless steels with helium ion irradiation. *J. Nucl. Mater.* 103: 445-450.

14. Prazak, M. and Eremias, B. 1972. A method for measuring the surface roughness factor of metals. *Corrosion Science* 12: 463-468.

15. Deev, G.F. 1986. Effects of carbon dioxide gas on the surface tension of molten metals. *Autom. Weld.* 39(6): 52-53.

Table 1

Compositions of JBK-75 Stainless Steels

Content (wt %)

	Chemical and Abrasive Experiments	Machining Experiments	Wire Brushing Experiments
Element	Heat A	Heat B	Heat C
Ni	30.0	29.7	30.8
Cr	14.3	13.9	15.6
Ti	2.0	2.1	2.0
Al	0.17	0.15	0.20
Mo	1.0	1.2	1.0
Mn	0.033	0.021	0.025
C	0.022	0.025	0.018
N	0.0045	0.001	0.0057
P	0.005	0.003	0.009
Si	0.060	0.024	0.052
V	0.23	0.21	0.23
B	0.0015	0.0004	0.0018
S	0.0022	0.004	0.0046
O	0.0021	0.001	0.0044
Fe	Balance	Balance	Balance

Table 2

Chemical and abrasive methods employed

Chemical Surface Preparations

1. Acid cleaning*
   A. Nitric acid (20 vol. %, room temperature, 6.25 min), distilled water rinse, nitric acid (30 vol. %)/Nitradd (20 vol. %) (38 °C, 6.25 min), distilled water rinse.
   B. Nitric acid (25 vol. %, room temperature, 6.25 min), distilled water rinse, nitric acid (35 vol. %)/Nitradd (25 vol. %) (43 °C, 6.25 min), distilled water rinse.
   C. Nitric acid (30 vol%)/Nitradd (20 vol. %) (38 °C, 6.25 min), distilled water rinse, nitric acid (20 vol. %, room temperature, 6.25 min), distilled water rinse.
   D. Nitric acid (20 vol. %, room temperature, 6.25 min), distilled water rinse.

2. Acid cleaning followed by solvent cleaning*. (Acid cleaning by method 1A above.)
   A. Vapor degrease in freon (5 min) followed by 1,1,1-trichloroethane (10 min).
   B. Aqueous clean in detergent (Oakite®).
   C. Wipe with isopropyl alcohol.
   D. Wipe with acetone.

3. Solvent clean only
   A. Vapor degrease in freon (5 min) followed by 1,1,1-trichloroethane (10 min).
   B. Aqueous clean in detergent (Oakite®, see * below for conditions).

Abrasive Surface Preparations

1. Wire brush using an AISI Type 302 wire brush, in air.**

2. Grit blast using 180 grit silica particles, in air.**

* Prior to acid cleaning, surfaces were degreased in 2 vol. % Oakite® NST aluminum cleaner in distilled water at 55 °C for 5 min and rinsed in distilled water.

** Prior to abrasive preparation, surfaces were degreased (*) and acid cleaned by procedure 1A.

Table 3 - Machining Methods Employed and Resultant Surface Finishes (Including Post-Machining Surface Treatment Conditions)

1. Lathe Turning - 63 Microinch Finish
   - A. Machined, Acid Cleaned
   - B. Machined, Wire Brushed, Acid Cleaned
   - C. Machined, Acid Cleaned, Wire Brushed
2. Electrical Discharge Machining - 83 Microinch Finish
   - A. Machined, Acid Cleaned
   - B. Machined, Wire Brushed, Acid Cleaned
   - C. Machined, Acid Cleaned, Wire Brushed
3. Milling - 125 Microinch Finish
   - A. Machined, Acid Cleaned
   - B. Machined, Wire Brushed, Acid Cleaned
   - C. Machined, Acid Cleaned, Wire Brushed
4. Milling - 250 Microinch Finish
   - A. Machined, Acid Cleaned
   - B. Machined, Wire Brushed, Acid Cleaned
   - C. Machined, Acid Cleaned, Wire Brushed
5. Milling - 500 Microinch Finish
   - A. Machined, Acid Cleaned
   - B. Machined, Wire Brushed, Acid Cleaned
   - C. Machined, Acid Cleaned, Wire Brushed

Table 4 - Welding Conditions

Process: DCEN, Partial Penetration GTAW

Electrode: 0.093 in. (2.4 mm) diameter
Tungsten - 2% Thoriated
10 degree vertex angle
0.031 in. (0.8 mm) truncation diameter

Electrode Extension: 1.250 in. (30.5 mm) from collet
0.375 in. (9.5 mm) from gas cup

Torch Position: Vertical

Gas Flow Rate: 22 scfh at 30 psig

	CHEMICAL & ABRASIVE EXPERIMENTS			MACHINING EXPERIMENTS		WIRE BRUSHING EXPERIMENTS
Welding Procedures	1	2	3	4	5	6
Welding Position	1G Flat	1G Flat	1G (Pipe) Horizontal Rolled (Sample Rotated)	1G Flat	1G Flat	1G Flat
Surface Welded	Flat Face	Flat Face	Circumference	Flat Face	Flat Face	Flat Face
Type of Weld	Bead-on-Plate	Bead-on-Plate	Bead-on-Plate	Spot-on-Plate	Bead-on-Plate	Bead-on-Plate
Current, amps	130	130	150	140	140	130
Travel Speed, in./min. (mm/s)	2.0 (0.9)	2.0 (0.9)	5.0 (2.1)	----	2.0 (0.9)	2.5 (1.1)
Spot Weld Duration (sec)	----	----	----	60	----	----
Voltage, V (Automatic Voltage Control)	10.0	----	8.0	10.4	10.0	10.8
Starting Torch Position, in. (mm) (Torch Position Locked)	----	0.066 (1.7)	----	----	----	----
Torch Shielding Gas Composition	25% Ar-75% He	25% Ar-75% He	100% Ar	25% Ar-75% He	25% Ar-75% He	25% Ar-75% He

Figure Captions

Fig. 1. Weld cross sections from welding procedure 1, 8.75X. (a) Chemical surface preparation (acid cleaned), d/w = 0.414; (b) Abrasive surface preparation (acid cleaned, then wire brushed), d/w = 0.660.

Fig. 2. Weld penetration for chemical and abrasive surface preparations. (a) Welding procedure 1, arc voltage 10.0 V, Ar-He; (b) Welding procedure 2, arc length 0.066 in., Ar-He; (c) Welding procedure 3, arc voltage 8.0 V, 100% Ar, circumferential weld; (d) Surface oxide thickness.

Fig. 3. Average arc voltage - arc length relationships.

Fig. 4. Effects of surface finish on spot weld d/w ratios (welding procedure 4).

Fig. 5. Weld profiles of bead-on-plate welds produced with welding procedure 5 on 125 microinch finish samples, 6.5X. (a) Machined and acid cleaned (condition A), d/w = 0.395; (b) Machined, wire brushed, and acid cleaned (condition B), d/w = 0.392; (c) Machined, acid cleaned, and wire brushed (condition C), d/w = 0.626.

Fig. 6. Relationship between d/w ratio and amount of wire brushing in air and in argon. Welding procedure 6, Ar-He.

Fig. 7. Cross sections of welds on JBK-75 with various levels of wire brushing, 10X. Welding procedure 6. (a) Unbrushed, d/w = 0.577; (b) Brushed 4 passes, d/w = 0.630; (c) Brushed 8 passes, d/w = 0.893; (d) Brushed 50 passes, d/w = 0.786.

Fig. 8. Relationship between weld dimensions and amount of wire brushing.

Fig. 9. Top views of welds on JBK-75 with various levels of wire brushing, 1.3X. Welding procedure 6. (a) Unbrushed; (b) Brushed 4 passes; (c) Brushed 8 passes; (d) Brushed 50 passes.

Fig. 10. Still photographs taken from laser-enhanced video of welds, 4.8X. Arc light is filtered out, revealing only weld pool and electrode tip. (a) Weld on acid cleaned, unbrushed, surface; (b) Weld on surface wire-brushed 2 times.

Fig. 11. Relationship between weld d/w ratio, surface oxide thickness, and surface roughness.

Fig. 12. Scanning electron micrographs of wire brushed surfaces, 100X. (a) Unbrushed; (b) Brushed 4 passes; (c) Brushed 8 passes; (d) Brushed 50 passes. 100X

Fig. 13. Weld d/w ratio versus torch gas oxygen content [3].

Fig. 14. Cross sections of full penetration welds on acid cleaned, unbrushed, JBK-75 base metal using two different spools of JBK-75 filler wire, 8X. The wire was from the same heat, but had different surface oxide thickness. (a) Wire oxide thickness 76 Å; (b) Wire oxide thickness 133 Å.

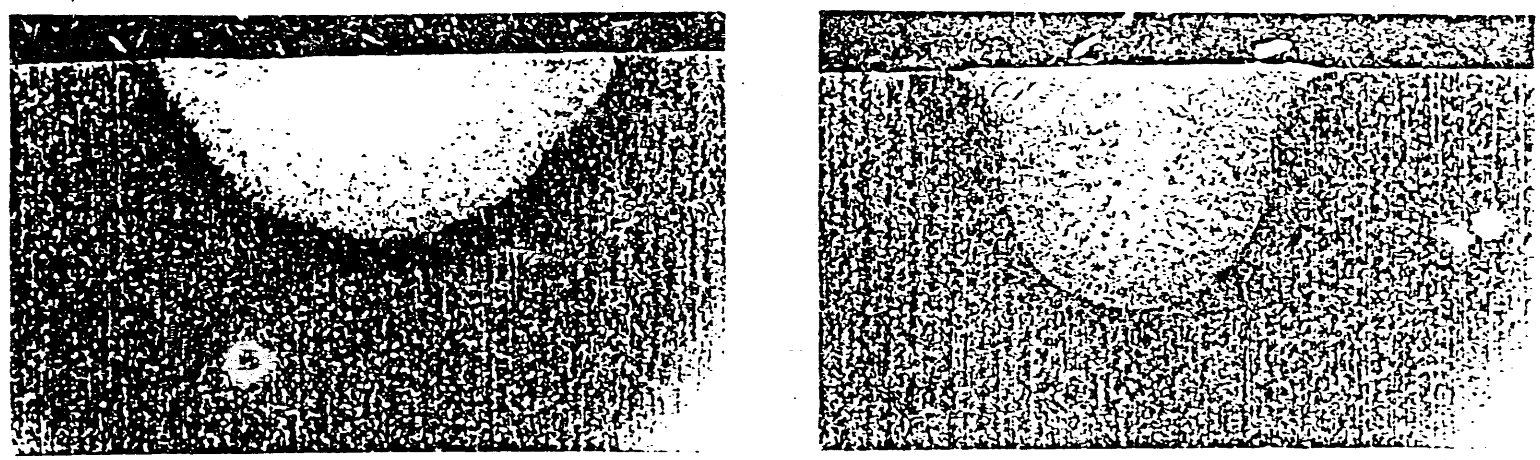

a. Chemical Surface Preparation (Acid Cleaned) D/W = 0.414

b. Abrasive Surface Preparation (Acid Cleaned Plus Wire Brushed) D/W = 0.660

Figure 1. Weld Cross Sections from Welding Procedure 1. 8.75X Magnification.

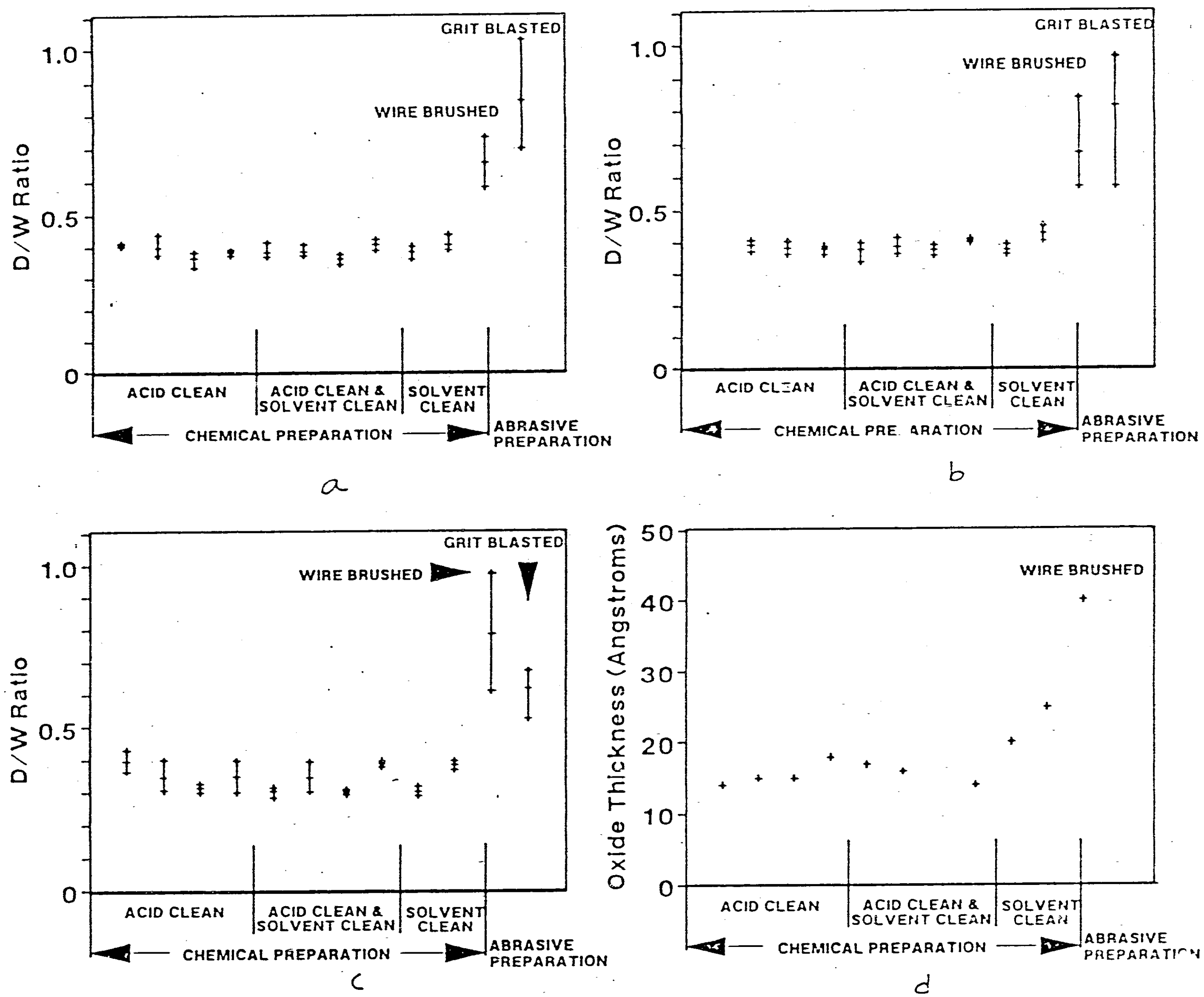

Fig. 2. Weld penetration for chemical and abrasive surface preparations. (a) Welding procedure 1, arc voltage 10.0 V, Ar-He; (b) Welding procedure 2, arc length 0.066 in., Ar-He; (c) Welding procedure 3, arc voltage 8.0 V, 100% Ar, circumferential weld; (d) Surface oxide thickness.

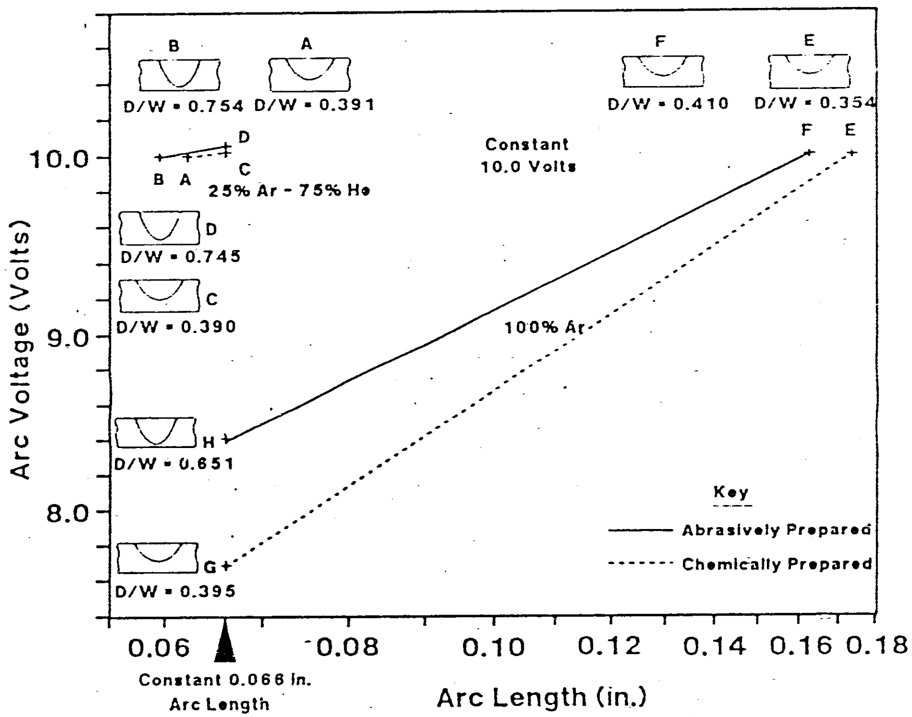

Fig. 3. Average arc voltage - arc length relationships.

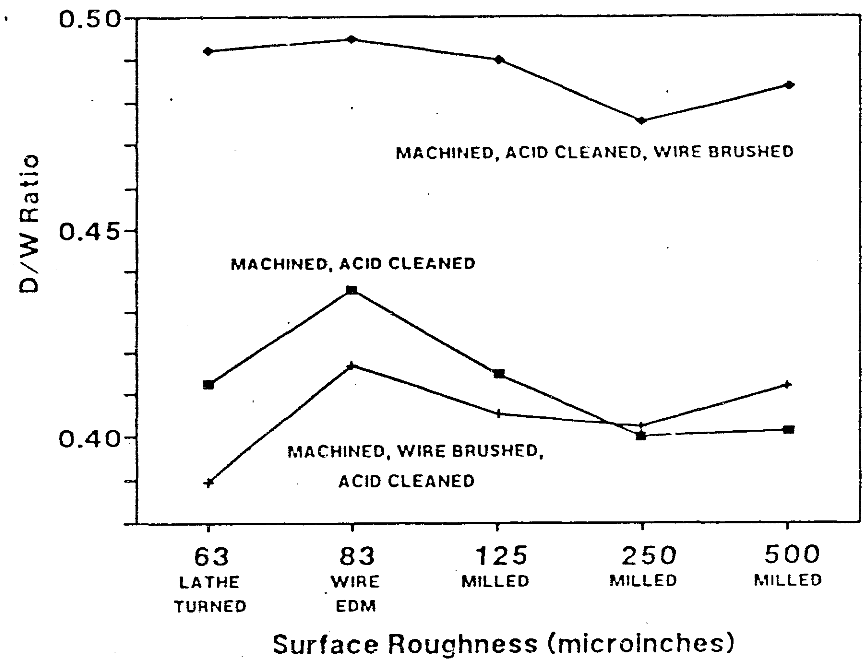

Fig. 4. Effects of surface finish on spot weld d/w ratios (welding procedure 4).

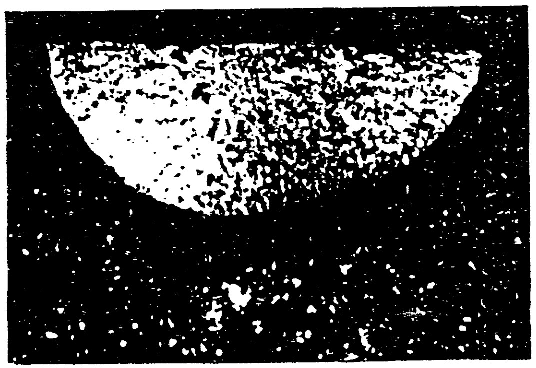

a. Machined and Acid Cleaned (Condition A)
D/W = 0.395

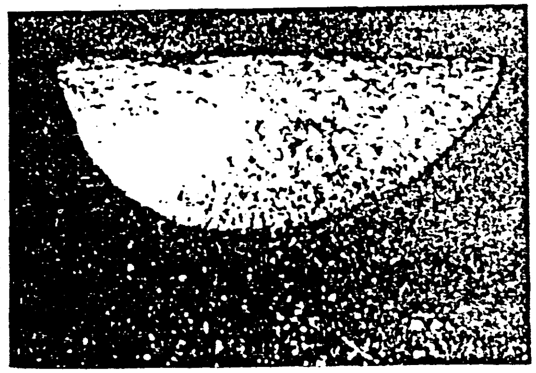

b. Machined, Wire Brushed, and Acid Cleaned (Condition B)
D/W = 0.392

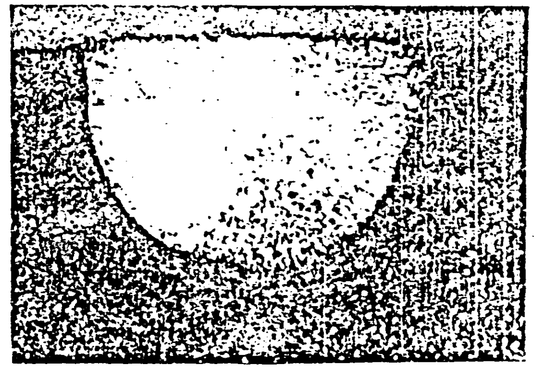

c. Machined, Acid Cleaned, and Wire Brushed (Condition C)
D/W = 0.626

Figure 5. Weld profiles of bead-on-plate welds produced with welding procedure 5 on 125 microinch finish samples. 6.5X magnification.

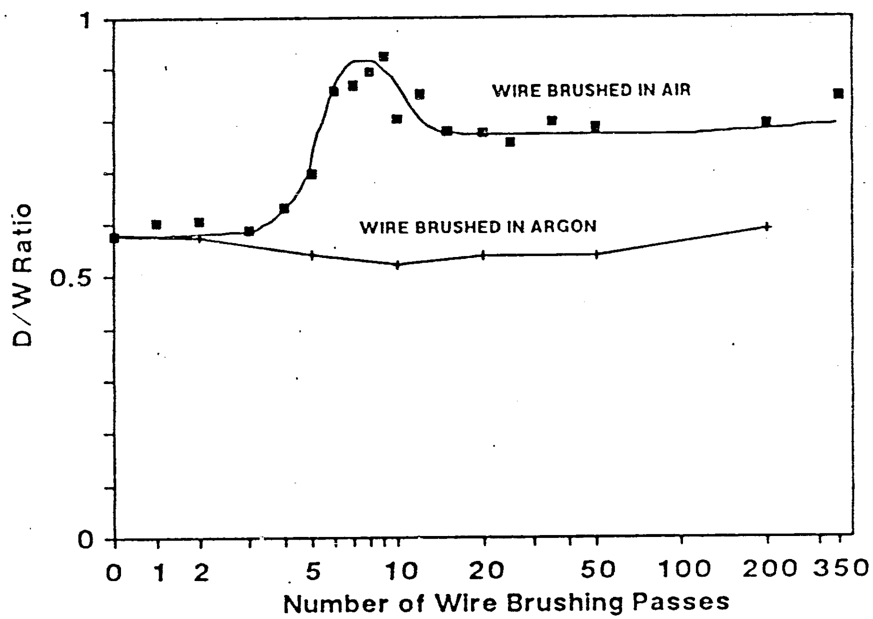

Fig. 6. Relationship between d/w ratio and amount of wire brushing in air and in argon. Welding procedure 6, Ar-He.

FIG 6

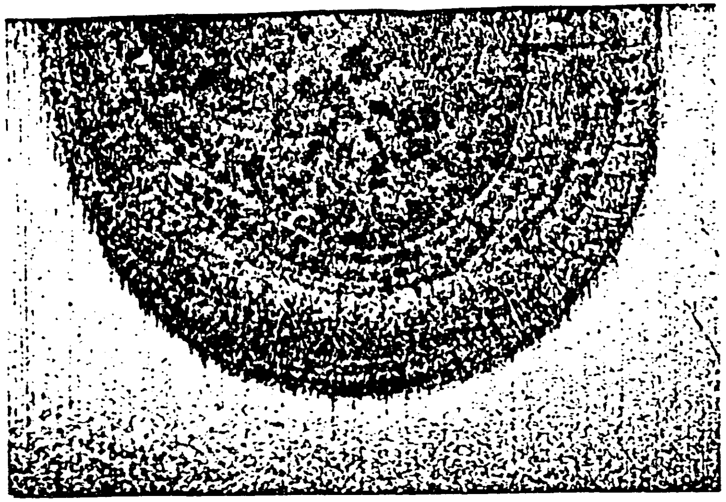

a. (Unbrushed)
D/W = 0.577

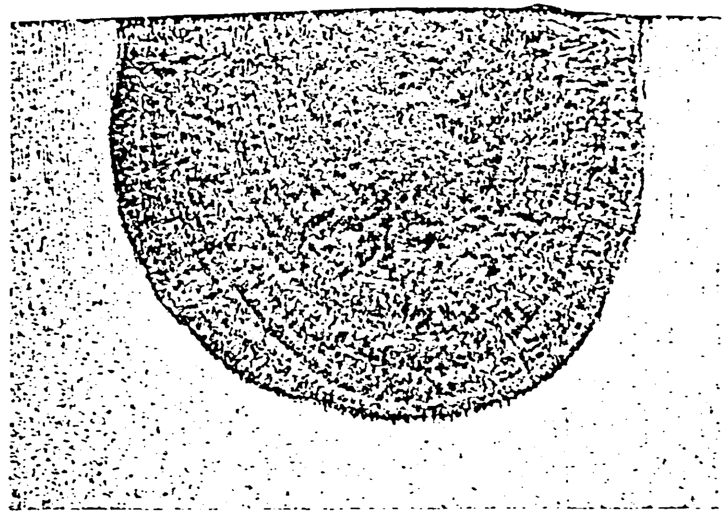

b. Brushed 4 Passes
D/W = 0.630

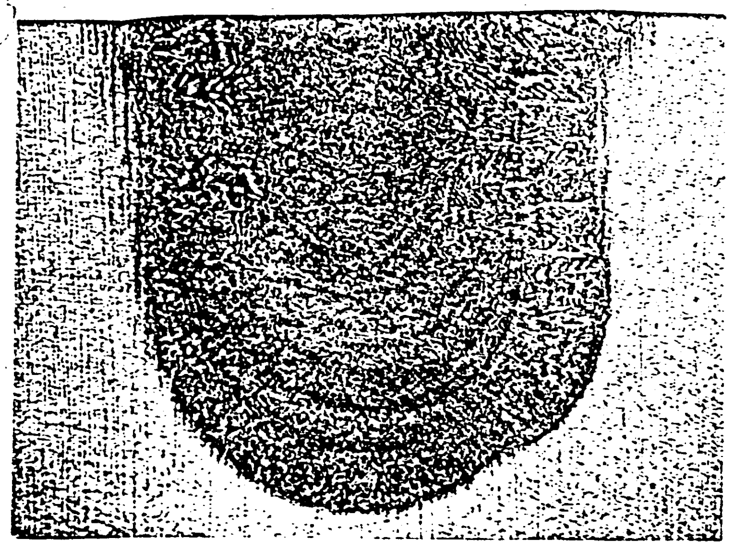

c. Brushed 8 Passes
D/W = 0.893

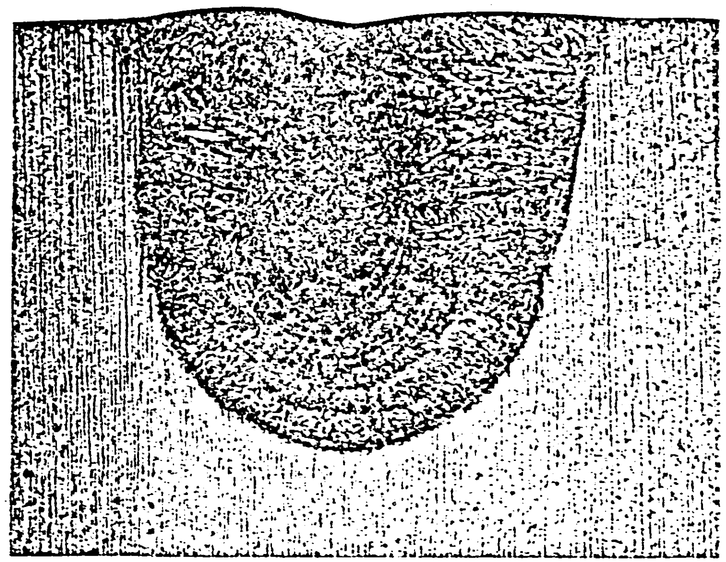

d. Brushed 50 Passses
D/W = 0.786

Figure 7. Cross sections of welds on JBK-75 with various levels of wire brushing using welding procedure B. 10X magnification.

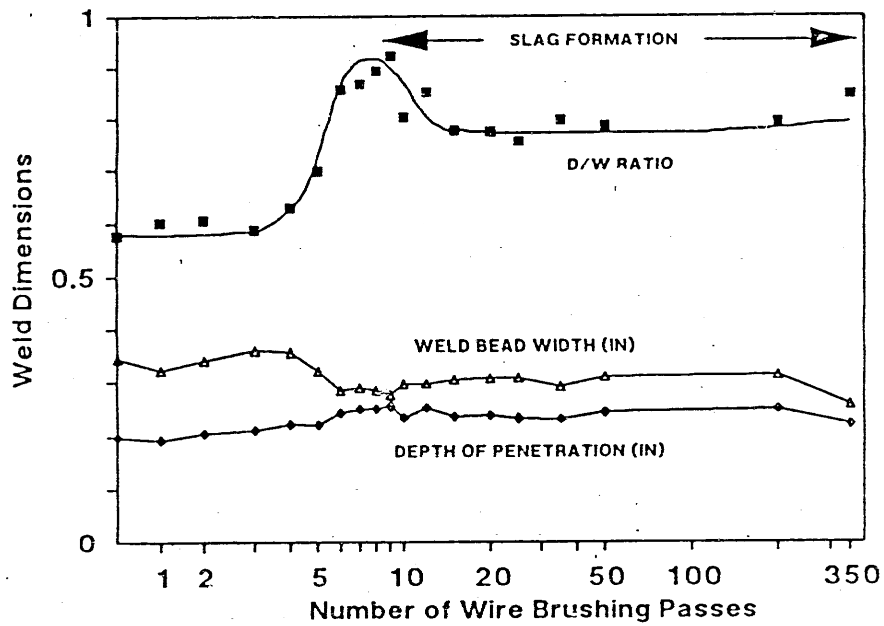

Fig. 8. Relationship between weld dimensions and amount of wire brushing.

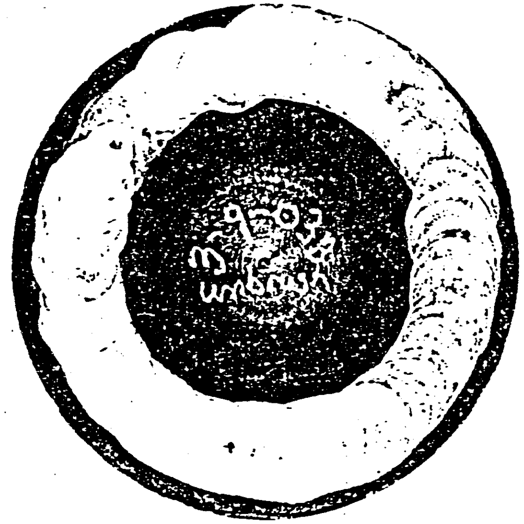

a. Acid Cleaned-(Unbrushed)

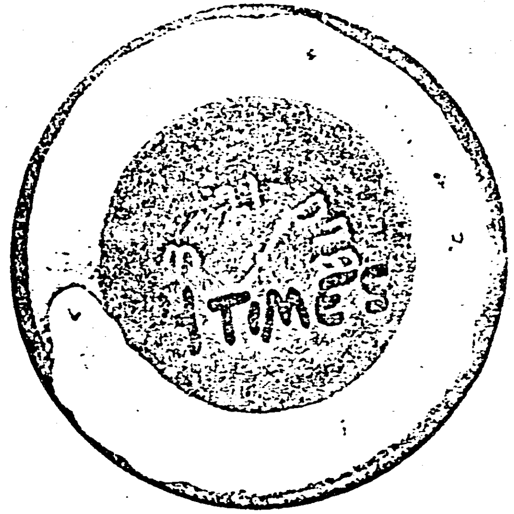

b. Brushed 4 Passes

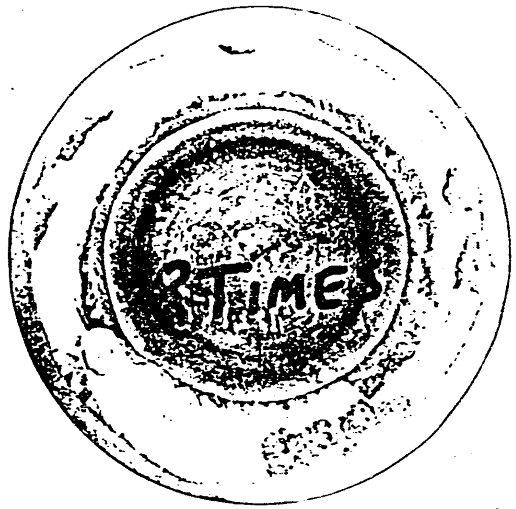

c. Brushed 8 Passes

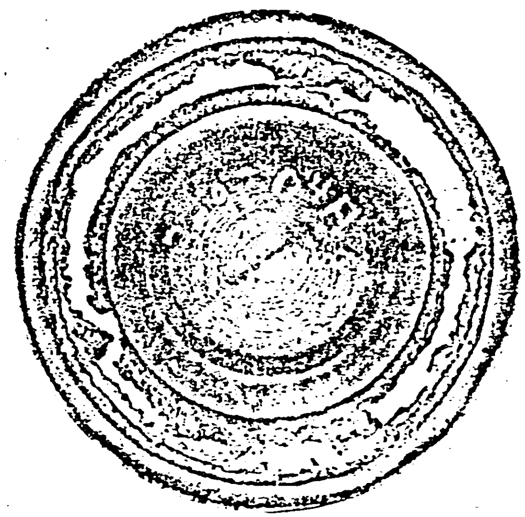

d. Brushed 50 Passses

Figure 9. Top views of welds on JBK-75 with various levels of wire brushing using welding procedure 8. 1.3X magnification.

a. Weld on acid cleaned (unbrushed) surface.

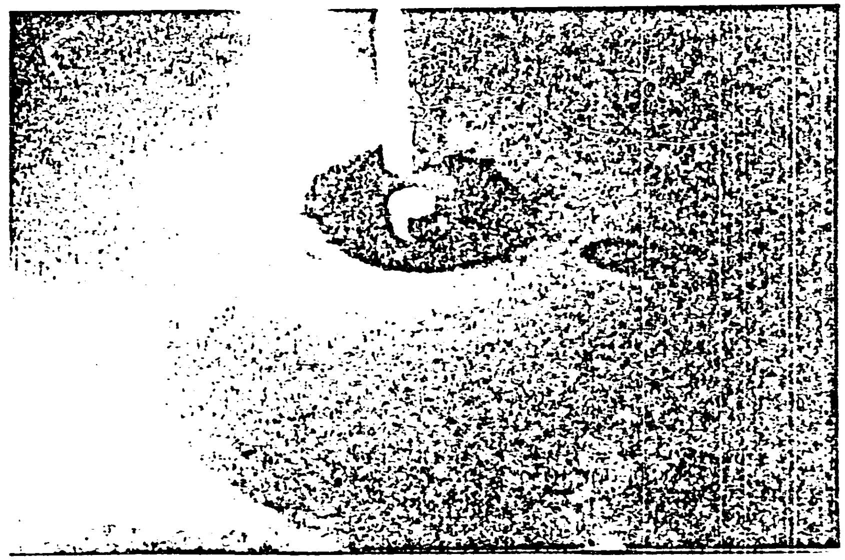

b. Weld on sample wire brushed 2 times.

Figure 10. Still photographs taken from laser-enhanced video of welds. Arc light is filtered out, revealing only weld pool and electrode tip. 4.8X magnification.

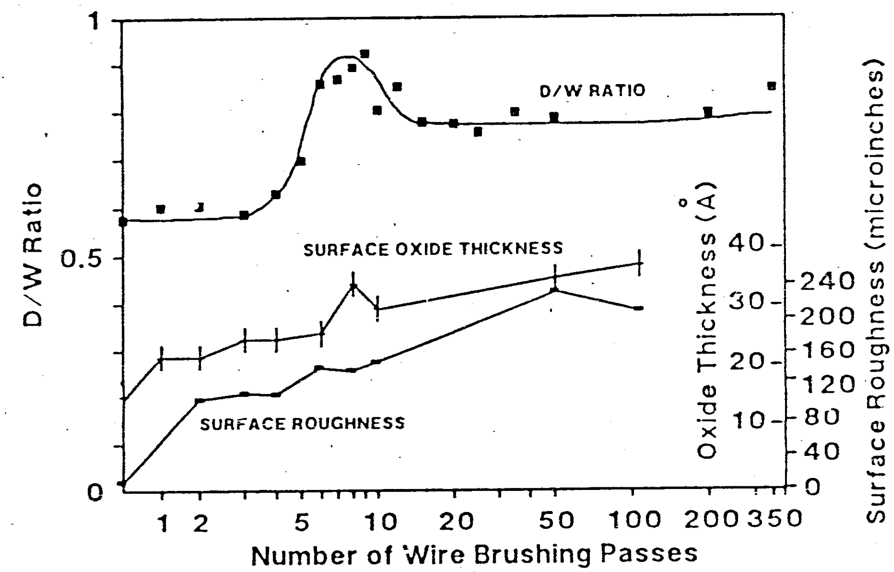

Fig. 11. Relationship between weld d/w ratio, surface oxide thickness, and surface roughness.

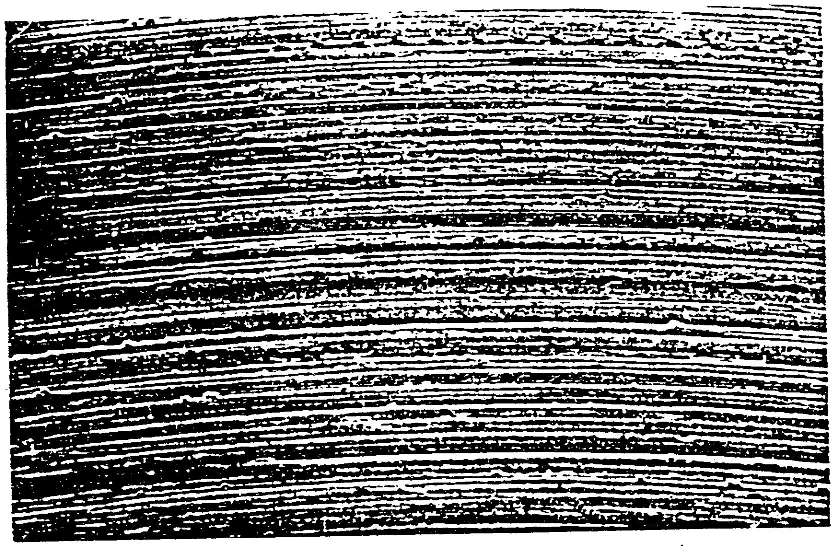

a. Acid Cleaned (Unbrushed)

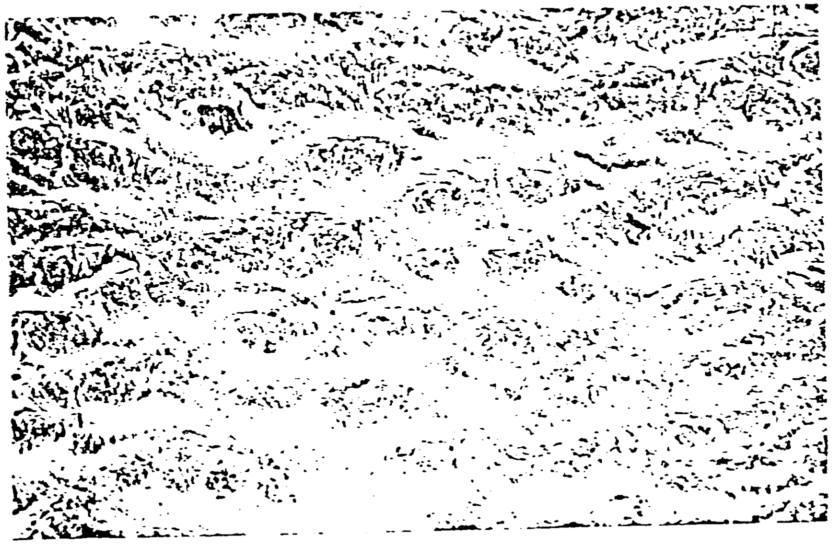

b. Brushed 4 Passes

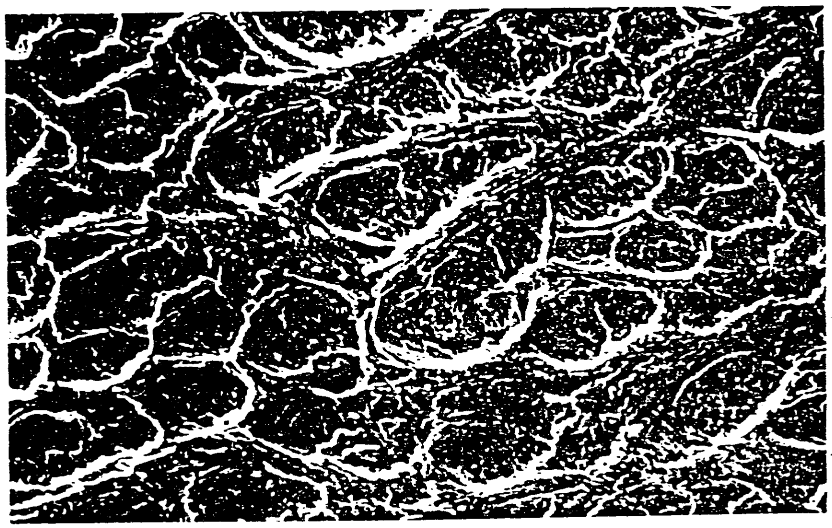

c. Brushed 8 Passes

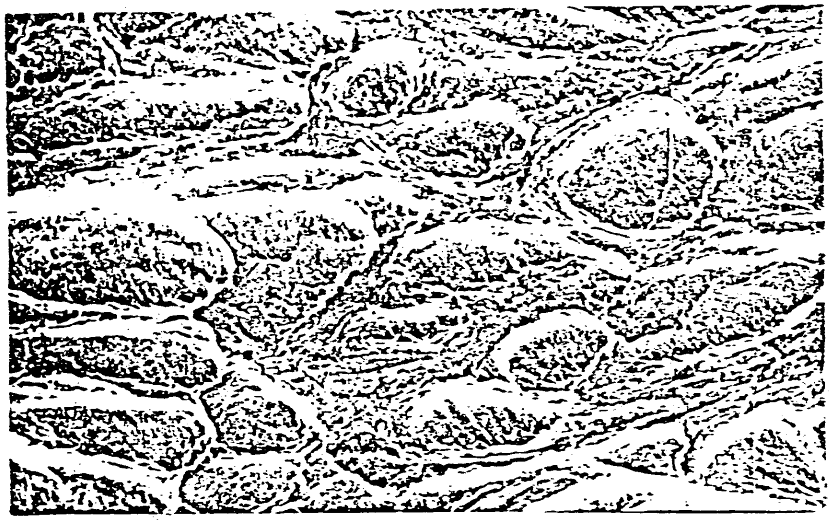

d. Brushed 50 Passses

Figure 12. Scanning electron micrographs of wire brushed surfaces. 100X magnification.

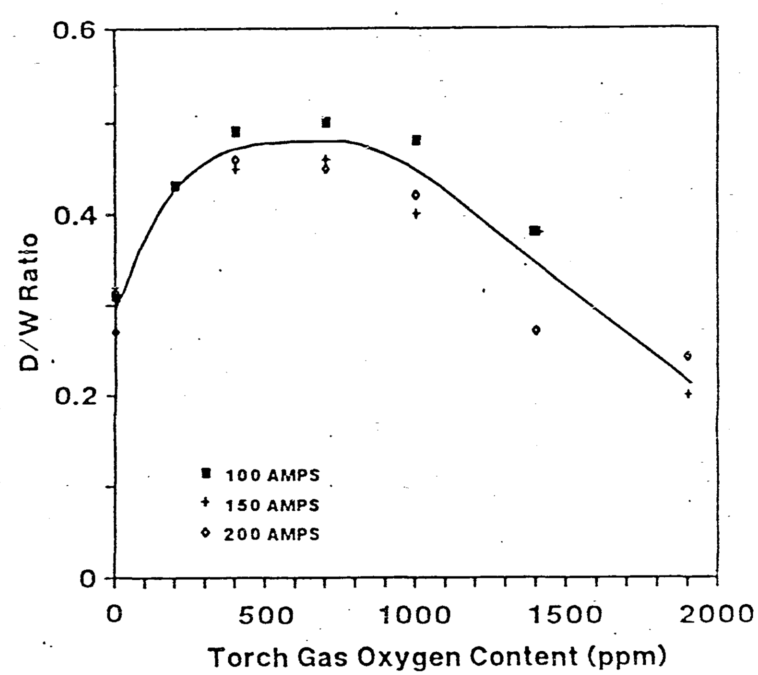

Fig. 13. Weld d/w ratio versus torch gas oxygen content [3].

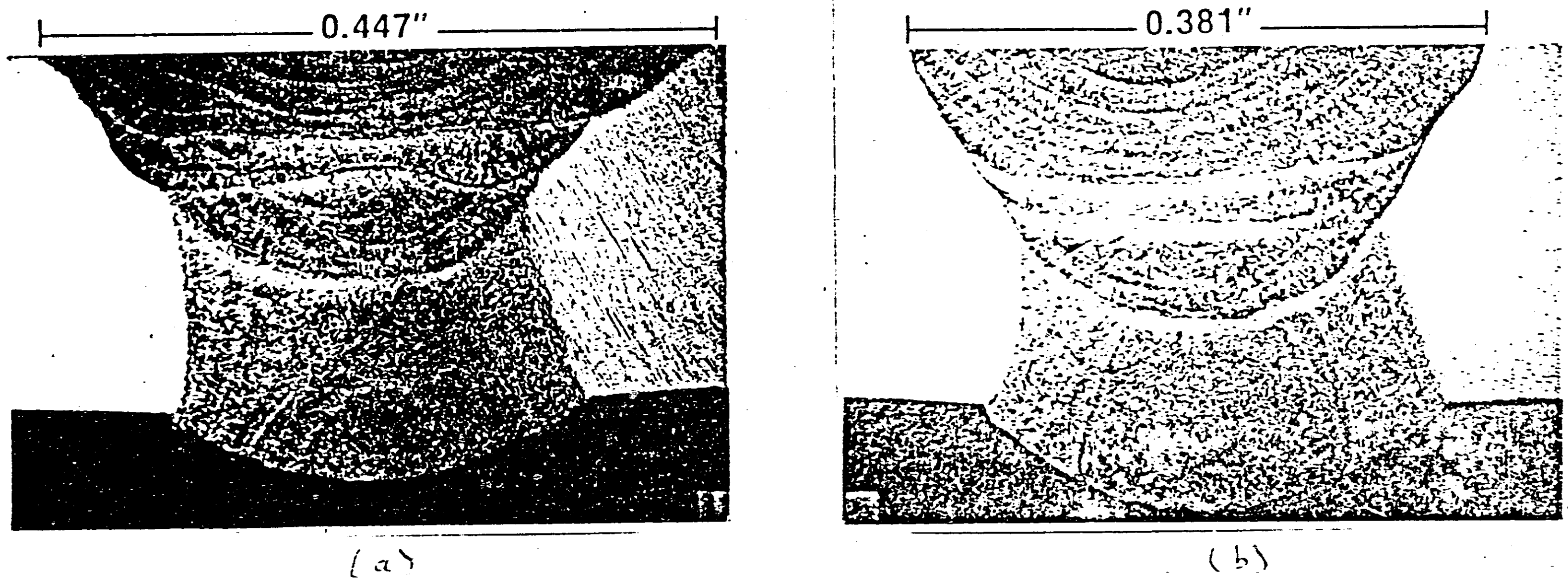

Fig. 14. Cross sections of full penetration welds on acid cleaned, unbrushed, JBK-75 base metal using two different spools of JBK-75 filler wire, 8X. The wire was from the same heat, but had different surface oxide thickness. (a) Wire oxide thickness 76 Å; (b) Wire oxide thickness 133 Å.

END

DATE FILMED

02 / 22 / 91